Circularly Polarized Light Emission from Semiconductor Planar Chiral Nanostructures

Kuniaki Konishi,[1,2] Masahiro Nomura,[3,4] Naoto Kumagai,[3] Satoshi Iwamoto,[3,4] Yasuhiko Arakawa,[3,4] and Makoto Kuwata-Gonokami[1,2,5,*]

[1]*Photon Science Center, The University of Tokyo, 7-3-1 Hongo, Bunkyo-ku, Tokyo 113-8656, Japan*
[2]*Department of Applied Physics, The University of Tokyo and CREST-JST, Hongo, Tokyo 113-8656, Japan*
[3]*Institute for Nano Quantum Information Electronics, The University of Tokyo, Komaba, Tokyo 153-8505, Japan*
[4]*Institute of Industrial Science, The University of Tokyo, Komaba, Tokyo 153-8505, Japan*
[5]*Department of Physics, The University of Tokyo, Hongo, Tokyo 113-0033, Japan*

(Received 30 January 2010; revised manuscript received 29 December 2010; published 1 February 2011)

We demonstrate circularly polarized light emission from InAs quantum dots embedded in the waveguide region of a GaAs-based chiral nanostructure. The observed phenomenon originates due to a strong imbalance between left- and right-circularly polarized components of the vacuum field and results in a degree of polarization as high as 26% at room temperature. A strong circular anisotropy of the vacuum field modes inside the chiral nanostructure is visualized using numerical simulation. The results of the simulation agree well with experimental results.

DOI: 10.1103/PhysRevLett.106.057402 PACS numbers: 78.67.Pt, 42.25.Ja, 42.50.Pq, 81.05.Xj

The polarization and intensity of the light emitted from a material depends on the internal structure of the source as well as on the symmetry and density of environmentally allowed electromagnetic modes. The role of the environment in light emission can be visualized by placing a light emitter in a microcavity [1–5]. The modification of the mode structure in the microcavity relative to that in free space affects the spontaneous emission rate. Similarly, the modification of the mode structure can also affect the radiation pattern and direction [6,7] of the emitted light. The polarization sensitivity of the spontaneous emission enables the polarization plane azimuth of a surface-emitting device to be controlled [8,9], and also offers important fundamental insights.

In particular, broken time-reversal symmetry results in different emission efficiencies for left- and right-circularly polarized photons in the presence of a static magnetic field [10–14]. A similar imbalance between the left- and right-circularly polarized photons may be expected in chiral media when left- and right-circularly polarized electromagnetic modes of the vacuum field are not equivalent. For example, it has been reported that spontaneous emission from dyes in chiral liquid crystals shows strong circular anisotropy [15–17].

Such spontaneous emission control can contribute to the development of circularly polarized light sources, which are important for applications such as circular dichroism spectroscopy [18] and chiral synthesis [19,20] in biology and chemistry, spin state control in quantum information technology [21,22], and ultrafast magnetization control [23,24]. Control of the circularly polarized spontaneous emission in conventional achiral semiconductor materials by using a chiral morphology effect enables the creation of novel solid-state circularly polarized light-emitting devices by using state-of-the-art semiconductor fabrication processes.

In this study, we present a method to develop a circularly polarized light emitter based on control of balance between left- and right-circularly polarized vacuum electromagnetic modes in semiconductor periodic nanostructures. These nanostructures are composed of unit cells having chiral morphology, which we call a ''chiral photonic crystal'' [25,26]. We design and fabricate a GaAs-based semiconductor chiral photonic crystal with an incorporated InAs quantum dot (QD) layer that produces circularly polarized photoluminescence (PL) at room temperature. A numerical simulation allows us to visualize the asymmetry of the vacuum modes coupled with circularly polarized light propagating along the surface normal. These results indicate that strong circularly polarized vacuum modes can be induced inside intrinsically achiral materials by fabricating chiral structures.

As shown in Fig. 1(a), a chiral photonic crystal consists of a GaAs gammadion layer, a GaAs waveguide-core layer incorporating an emitter layer with InAs QDs, and an $Al_{0.7}Ga_{0.3}As$ clad layer on a GaAs substrate. The gammadion layer acts as a clad layer with lower effective refractive index than GaAs, and a waveguide is formed [25,26]. The thickness of the gammadion, waveguide-core, and clad layers are 460 nm, 260 nm, and 1 μm, respectively. The GaAs gammadion layer consists of structures that have no in-plane mirror symmetry but possess a fourfold rotational axis. Such on-waveguide planar chiral structures possess strong optical activity [25–27]. The period of the gammadion array is 1290 nm $\times$ 1290 nm. We prepared three samples with different linewidths (α, β) of (146 nm, 610 nm), (177 nm, 626 nm), and (200 nm, 638 nm), as shown in Fig. 1(a) [28].

We visualize chirality of the manufactured structures by measuring the polarization plane azimuth rotation θ and ellipticity ψ of the transmitted light wave at normal

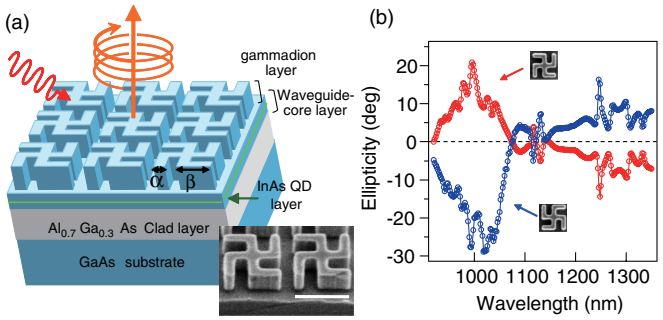

FIG. 1 (color online). (a) Schematic of designed chiral nanostructure. Gammadion and waveguide-core layers are fabricated of GaAs. Typical scanning electron microscopy image of a chiral photonic crystal with a left-twisted gammadion is also shown. Length of white scale bar corresponds to 1 μm. Values of the indicated structural parameters are given in the text. (b) Measured ellipticity spectra in the zero-order transmitted light of the chiral photonic crystals. Gray (red) [black (blue)] line indicates the result obtained with the left- [right-]twisted gammadion sample.

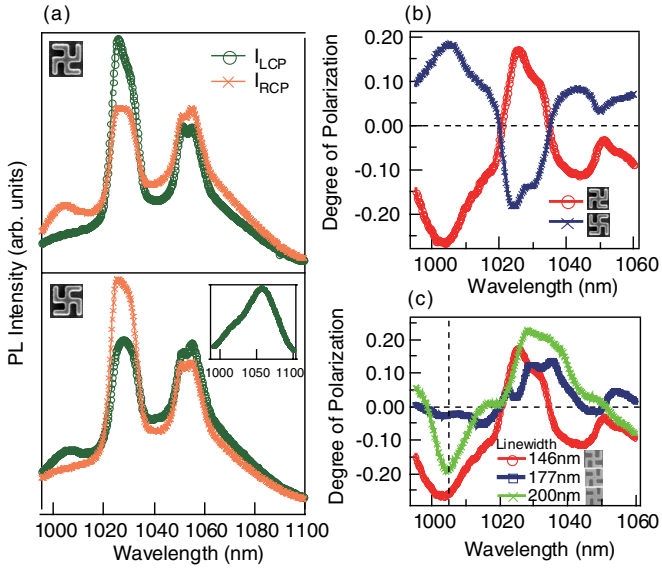

FIG. 2 (color online). Left- (I_{LCP}) and right-circularly polarized (I_{RCP}) components of PL spectra from left-twisted (top) and right-twisted (bottom) chiral photonic crystals with a linewidth $\alpha = 146$ nm. Inset shows PL spectra without nanostructures. (b) Spectra of the DOP of chiral photonic crystals with left- gray (red) line] and right-twisted [black (blue) line] gammadions with a linewidth $\alpha = 146$ nm. (c) Spectra of the DOP of chiral photonic crystals with different linewidths. Broken line indicates wavelength of 1004 nm.

incidence using a conventional polarization modulation technique [29]. The transmission spectra for left- and right-twisted gammadion structures are nearly identical, and the signs of both θ and ψ are opposite at all wavelengths. Figure 1(b) shows ellipticity spectra for left- and right-twisted gammadion structures. As we have reported in Ref. [25], optical activity is enhanced at the wavelengths of waveguide resonances depending on the period of arrayed structures, which are clearly observed at approximately 1260 and 1150 nm. In particular, greater optical activity is observed at shorter wavelengths where several higher-order waveguide modes, which correspond to $m_x^2 + m_y^2 = 16, 17, 18$ [30], overlap between 950 and 1100 nm. The fluctuations observed in this region are considered to arise due to interference between waveguide resonances and resonances inside the gammadion structure.

We measure the PL of the chiral nanostructures along the sample normal (numerical aperture $\sim$0.03) [28] for details of the measurement). Figure 2(a) shows that the PL spectra of the InAs QDs incorporated into the chiral nanostructure differ considerably for left- (I_{LCP}) and right-circularly polarized (I_{RCP}) components. For comparison, the PL spectra of InAs QDs without chiral nanostructures are shown in the inset of Fig. 2(a). Strong left-right PL asymmetry is observed between 1000 and 1060 nm. Large ellipticity is also observed in the transmission measurement in this region [Fig. 1(b)]. The PL spectrum of the left- (right-)circularly polarized component from the left-twisted gammadion sample matches that of the right-(left-)circularly polarized component from the right-twisted sample. This shows that helicity of the emitted light depends on whether the chiral nanostructures are left or right twisted. The wavelength dependence of the degree of polarization (DOP) of the emitted light $P \equiv (I_{\mathrm{LCP}} - I_{\mathrm{RCP}})/(I_{\mathrm{LCP}} + I_{\mathrm{RCP}})$ from left- and right-twisted samples is shown in Fig. 2(b). Figure 2(c) shows $P = -26.4\%$ at 1004 nm for the left-twisted sample with a linewidth $\alpha = 146$ nm, whereas the DOP spectra depend strongly on the gammadion linewidth.

Note that the DOP spectra [Fig. 2(b)] and transmission polarization spectra [Fig. 1(b)] clearly differ. This indicates that the observed circularly polarized emission is not simply explained as a result of polarization-dependent propagation of photons radiated from the QDs through the gammadion layer. The observed left-right asymmetry of the PL can be explained in terms of the strong left-right imbalance of the vacuum electromagnetic field due to the presence of the chiral nanostructure. Spontaneous emission can be seen as radiative transition induced by the vacuum electromagnetic fields. In the framework of this approach, quantum electrodynamics effects, which modify spontaneous emissions in the nanostructures, can be considered as a result of renormalization of the allowed field modes. We now consider a light emitter placed in a lossless dielectric microstructure; the emission signal is observed far from the structure. We can decompose the electromagnetic field in the system, consisting of a chiral nanostructure, a GaAs substrate, and free space, into orthogonal modes that can be described by electric field $\boldsymbol{E}_{\boldsymbol{k}\lambda}(\boldsymbol{r})$, where $\boldsymbol{k}$ is the wave vector in the free-space region, subscript $\lambda = L$ or R denotes light- or right-circular polarizations, respectively, and $\boldsymbol{r}$ is the position. The vacuum field amplitude of each

mode $|\boldsymbol{E}_{k\lambda}(\boldsymbol{r})| = \sqrt{\langle \boldsymbol{E}^{\dagger}_{k\lambda}(\boldsymbol{r})\boldsymbol{E}_{k\lambda}(\boldsymbol{r})\rangle_{\mathrm{vac}}}$ determines the rate $\eta_{k\lambda}(\boldsymbol{r})$ of spontaneous emission into a free-space propagation mode with wave vector $\boldsymbol{k}$ and polarization λ: $\eta_{k\lambda}(\boldsymbol{r}) = \frac{2\pi}{\hbar^2}|\boldsymbol{\mu}|^2|\boldsymbol{E}_{k\lambda}(\boldsymbol{r})|^2\delta(\omega_0 - \omega_{k\lambda})$, where $\boldsymbol{\mu}$ is the in-plane dipole moment of a radiation source assuming random orientation, ω_0 is the resonance frequency, and $\omega_{k\lambda}$ is the frequency of the vacuum field mode. In the PL experiment, we measured the intensity of the DOP of spontaneous emission along the normal to the substrate, which is proportional to the difference between $\eta_{kL}(\boldsymbol{r})$ and $\eta_{kR}(\boldsymbol{r})$. Thus, the obtained value of P is a quantitative measure of the left-right asymmetry of the vacuum field in the chiral nanostructure.

In linear optics, the electric field of a light wave at a frequency ω at a point $\boldsymbol{r}$ near the nanostructure $\boldsymbol{E}^t(\boldsymbol{r})$ is a linear function of the amplitude of the incident plane wave $\boldsymbol{E}^{\mathrm{in}}(\boldsymbol{r}) = \boldsymbol{A}e^{i\boldsymbol{k}_0\cdot\boldsymbol{r}}$, given as

$$E^t_i(\boldsymbol{r}) = l_{ij}(\boldsymbol{r}, \boldsymbol{k}_0)A_j e^{i\boldsymbol{k}_0\cdot\boldsymbol{r}}, \tag{1}$$

where $\boldsymbol{k}_0$ is the wave vector of the incident plane wave, subscripts indicate Cartesian coordinates, and $l_{ij}(\boldsymbol{r}, \boldsymbol{k}_0)$ is a tensorial function that depends on the structure's material properties and geometry. Because plane waves are eigenmodes of free space, this equation can be employed to visualize how the inhomogeneity modifies the mode structure of the medium. In particular, if we consider a mode that connects to a plane wave which propagates with a wave vector $\boldsymbol{k}_0$ and has vacuum field amplitude of free space at large distance from the structure, the tensorial function $l_{ij}(\boldsymbol{r}, \boldsymbol{k}_0)$ can be considered to be a measure of the enhancement or suppression of the spontaneous emission rate of that mode at the point $\boldsymbol{r}$.

If the planar structure is isotropic in the XY plane, symmetry yields $l_{ij}(\boldsymbol{r}, \boldsymbol{k}_0) = l(\boldsymbol{r})\delta_{ij}$. The magnitudes of the left- and right-circularly polarized vacuum modes coupled with light propagating along the structure normal are given by $E^t_{L,R}(\boldsymbol{r}) = l_{L,R}(\boldsymbol{r})A_{L,R}$. In an isotropic chiral layer, the counter-circularly polarized vacuum modes will be modified differently. Thus, if a dipole oscillator emits left- and right-circularly polarized photons equally in a homogeneous medium (i.e., $|\boldsymbol{A}_L| = |\boldsymbol{A}_R|$), the same dipole embedded in the chiral slab at point $\boldsymbol{r}$ emits radiation with a finite DOP given by

$$\xi(r) = \frac{|\eta_{k_0L}(\boldsymbol{r})| - |\eta_{k_0R}(\boldsymbol{r})|}{|\eta_{k_0L}(\boldsymbol{r})| + |\eta_{k_0R}(\boldsymbol{r})|} = \frac{|\boldsymbol{E}^t_L(\boldsymbol{r})|^2 - |\boldsymbol{E}^t_R(\boldsymbol{r})|^2}{|\boldsymbol{E}^t_L(\boldsymbol{r})|^2 + |\boldsymbol{E}^t_R(\boldsymbol{r})|^2} = \frac{|l_L(\boldsymbol{r})|^2 - |l_R(\boldsymbol{r})|^2}{|l_L(\boldsymbol{r})|^2 + |l_R(\boldsymbol{r})|^2}. \tag{2}$$

Thus, circular anisotropy of the vacuum field $\xi(\boldsymbol{r})$ in the chiral photonic structure can be visualized by comparing the light intensity at point $\boldsymbol{r}$ when the structure is irradiated by left- and right-circularly polarized plane waves with the same amplitude at normal incidence. When the QDs are homogeneously distributed in the XY plane at a given z, forming a two-dimensional emitter layer, the far-field plane wave emission normal to the surface shows a DOP characterized by

$$P(z) = \frac{\int[|l_L(\boldsymbol{r})|^2 - |l_R(\boldsymbol{r})|^2]dxdy}{\int[|l_L(\boldsymbol{r})|^2 + |l_R(\boldsymbol{r})|^2]dxdy}. \tag{3}$$

Figure 3(a) shows the calculated induced electric field distribution for left- and right-circularly polarized light with the same amplitude incident normally at a wavelength of 1004 nm, which features a large DOP [Fig. 2(b)]. We used the rigorous coupled-wave analysis method [31]. Figure 3(a) shows a drastic difference in the light intensity distribution for counter-circularly polarized incident waves $|l_L(\boldsymbol{r})|^2$ and $|l_R(\boldsymbol{r})|^2$. At this wavelength, only $|l_R(\boldsymbol{r})|^2$ is strongly enhanced inside the waveguide-core and gammadion layers. This difference represents the sensitivity of the vacuum field modes to the handedness of circularly polarized light. Figure 3(b) shows the in-plane distributions of $l_{L,R}(\boldsymbol{r})$ at $z = 570$ nm (corresponding to the position of the emitter layer); the calculated value of $P(z)$ is -27.4%. We also performed the same calculation for the different linewidth structures as shown in Figs. 3(b)–3(d). The calculated values of $P(z)$ agree well with the experimental data shown in Fig. 2(c). These figures show that the field distributions of only right-circularly polarized components are strongly enhanced and are sensitive to the linewidth of the gammadion patterns. Fourier transformed images of Fig. 3(b) (not shown) show dominant contribution of the waveguide mode, $(m_x, m_y) = (3, 3)$ [30]. As shown in Fig. 3(e), $P(z)$ is enhanced in the gammadion and waveguide-core layers, and the largest DOP can be achieved when the emitter layer is placed in the middle of the waveguide-core layer, where the electric field is strongly enhanced, as shown in Fig. 3(a).

Our analysis shows that the DOP of light emitted by a QD can be controlled by selecting its position in the structure. For example, if we place a single emitter in the center of the gammadion, as indicated by the white arrows in Fig. 3(a), the DOP of the emitted light will be as large as 91%. This indicates that this new method can realize a circularly polarized emitter with thinner structures than conventional liquid crystal systems, which are typically several microns thick. In our system, such precise control of the structure and position of the radiation source should be possible because the structures are fabricated using a top-down approach in semiconductor fabrication technologies, unlike a conventional system of dyes in chiral liquid crystals. Thus, this method possesses a new degree of freedom for designing circularly polarized emitters, which suggests applications such as a novel circularly polarized single photon source and a surface-emitting circularly polarized laser.

In conclusion, we demonstrate a system that possesses left-right circular polarization asymmetry of the vacuum electromagnetic modes and observe a pronounced

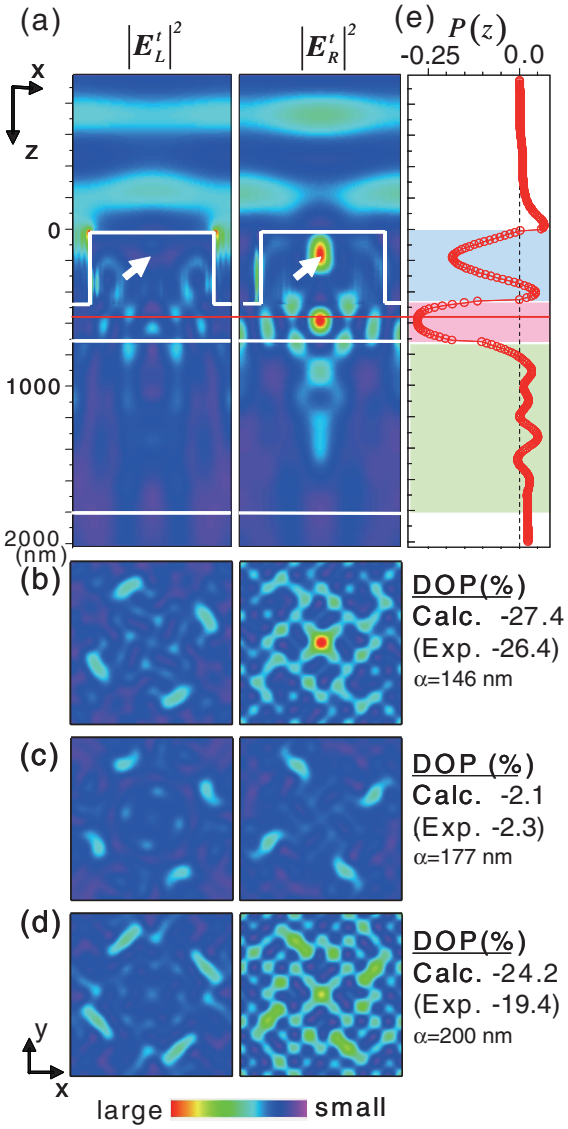

FIG. 3 (color). (a) Distribution of electric field intensity induced by left- and right-circularly polarized light with the same amplitude ($|E_L^t|^2$ and $|E_R^t|^2$, respectively) at normal incidence tuned to 1004 nm, sliced on the xz plane including the center of the sample with a 146 nm linewidth. Substrate is modeled as a semi-infinite slab of GaAs. White lines indicate interfaces of the GaAs layer. (b)–(d) In-plane distribution of electric field intensity induced in samples with linewidths α of (b) 146 nm, (c) 177 nm, and (d) 200 nm by left- (left-hand side) and right-polarized (right-hand side) light at normal incidence. Vertical position of the calculated planes is 570 nm, as indicated by red lines in (a). Calculated and experimentally determined degrees of polarization are shown on the right. (e) Dependence of the DOP of sample with linewidth $\alpha = 146$ nm on the z position. Red line indicates position of emitter layer. Blue, red, and green areas indicate the gammadion, waveguide-core, and clad layers, respectively.

imbalance between left- and right-circular polarization in light emitted by QDs embedded in a chiral photonic crystal. The obtained DOP of the PL spectra is as large as 26%. This optimal control of the DOP by introducing left-right asymmetry in the vacuum field is important for various applications, including quantum information technology.

We appreciate H. Tamaru, Y. Svirko, and J. B. Héroux for fruitful discussions, and are grateful to H. Ono, T. Sato, and T. Shimura for sample fabrication. This research is supported by the Photon Frontier Network Program, KAKENHI(20104002), Special Coordination Funds for Promoting Science and Technology of MEXT, Japan, and by JSPS through its FIRST Program.

*gonokami@phys.s.u-tokyo.ac.jp

[1] E. Yablonovitch, Phys. Rev. Lett. **58**, 2059 (1987).
[2] G. Björk, H. Heitmann, and Y. Yamamoto, Phys. Rev. A **47**, 4451 (1993).
[3] P. Lodahl *et al.*, Nature (London) **430**, 654 (2004).
[4] D. Englund *et al.*, Phys. Rev. Lett. **95**, 013904 (2005).
[5] H. Altug, D. Englund, and J. Vučkovič, Nature Phys. **2**, 484 (2006).
[6] E. Miyai *et al.*, Nature (London) **441**, 946 (2006).
[7] S. Fan, P. R. Villeneuve, J. D. Joannopoulos, and E. F. Schubert, Phys. Rev. Lett. **78**, 3294 (1997).
[8] S. Noda, M. Yokoyama, M. Imada, A. Chutinan, and M. Mochizuki, Science **293**, 1123 (2001).
[9] S. Strauf *et al.*, Nat. Photon. **1**, 704 (2007).
[10] R. Fiederling *et al.*, Nature (London) **402**, 787 (1999).
[11] Y. Ohno *et al.*, Nature (London) **402**, 790 (1999).
[12] E. I. Rashba, Phys. Rev. B **62**, R16 267 (2000).
[13] X. Jiang *et al.*, Phys. Rev. Lett. **94**, 056601 (2005).
[14] M. Holub and P. Bhattacharya, J. Phys. D **40**, R179 (2007).
[15] H. Stegemeyer, W. Stille, and P. Pollmann, Isr. J. Chem. **18**, 312 (1979)
[16] J. Schmidtke and W. Stille, Eur. Phys. J. B **31**, 179 (2003).
[17] K. L. Woon, M. O'Neill, G. J. Richards, M. P. Aldred, and S. M. Kelly, Phys. Rev. E **71**, 041706 (2005).
[18] L. D. Barron, *Molecular Light Scattering and Optical Activity* (Cambridge University Press, Cambridge, 1983).
[19] H. Rau, Chem. Rev. **83**, 535 (1983).
[20] Y. Inoue, Chem. Rev. **92**, 741 (1992).
[21] M. Kroutvar *et al.*, Nature (London) **432**, 81 (2004).
[22] J. Berezovsky *et al.*, Science **314**, 1916 (2006).
[23] H. Krenn, W. Zawadzki, and G. Bauer, Phys. Rev. Lett. **55**, 1510 (1985).
[24] D. D. Awschalom, J. Warnock, and S. von Molnār, Phys. Rev. Lett. **58**, 812 (1987).
[25] K. Konishi *et al.*, Opt. Express **16**, 7189 (2008).
[26] B. Bai *et al.*, Opt. Express **17**, 688 (2009).
[27] B. Bai, Y. Svirko, J. Turunen, and T. Vallius, Phys. Rev. A **76**, 023811 (2007).
[28] See supplemental material at http://link.aps.org/supplemental/10.1103/PhysRevLett.106.057402 for detailed information about sample fabrication, experimental setup, and calculation.
[29] M. Kuwata-Gonokami *et al.*, Phys. Rev. Lett. **95**, 227401 (2005).
[30] m_x and m_y are mode integers of waveguide with periodic structurer (see Ref. [25]).
[31] The number of harmonics used for rigorous coupled-wave analysis calculation is 16 [28].